ACS APPLIED MATERIALS & INTERFACES

LETTER

www.acsami.org

Enhanced Thermoelectric Properties of $Bi_{0.5}Sb_{1.5}Te_3$ Films by Chemical Vapor Transport Process

Zhengliang Sun,[†,‡] Shengcong Liufu,[†] Xihong Chen,[*,†] and Lidong Chen[†]

[†]CAS Key Laboratory of Materials for Energy Conversion, Shanghai Institute of Ceramics, Chinese Academy of Science, 1295 Dingxi Road, Shanghai 200050, PR China

[‡]Graduate School of the Chinese Academy of Science, 19 Yuquan Road, Beijing 100049, P.R. China

Supporting Information

ABSTRACT: $Bi_{0.5}Sb_{1.5}Te_3$ films were prepared by a novel chemical vapor transport process through delicate controlling the temperature of the substrate and vapor source. The power factor reaches 30 $\mu W\ cm^{-1}\ K^{-1}$ at room temperature, which is much higher than the value of the $Bi_{0.5}Sb_{1.5}Te_3$ films prepared by other techniques. The enhancement of thermoelectric properties might be attributed to the higher carrier mobility (252 $cm^2\ V^{-1}\ s^{-1}$), coming from the effective interparticle contiguity of (00*L*) oriented nanoplates embedded in the present $Bi_{0.5}Sb_{1.5}Te_3$ films.

KEYWORDS: thermoelectric, $Bi_{0.5}Sb_{1.5}Te_3$, film, chemical vapor transport, transport properties, nanoplate

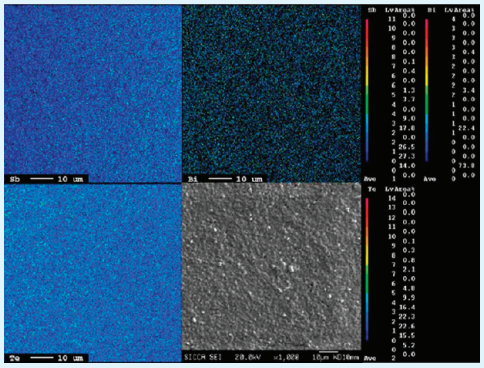

Thermoelectrics, in the form of films, have provided a potential platform to be integrated into electronic devices in the microheating and cooling areas.[1,2] The family of A_2B_3 (A = Bi, Sb and B = Te, Se) compounds possess excellent thermoelectric (TE) properties near room temperature and are predicted to be the best candidates for TE film devices.[3−8] Because binary A_2B_3 films can be easily obtained by either vacuum-based route[3] or solution-based route.[6,7] The corresponding TE properties and the way to enhance the TE properties of the A_2B_3 films have been widely studied. Among them, doping is an effective and mostly used method as the carrier concentration can be adjusted into an appropriate range even by a small doped amount. For example, an introduction of 10% Se into Bi_2Te_3 was reported to bring ∼30% enhancement of the power factor[8] (PF, defined as $S^2\sigma$, where S and σ are Seebeck coefficient and electrical conductivity, respectively). Besides, excess alloying scattering by the Se dopant will further decrease the thermal conductivity (κ), which will also contribute to the enhancement of the dimensionless figure of merit (ZT, expressed as $S^2\sigma T/\kappa$). In this work, the best p-type thermoelectric material near room temperature,[9] $Bi_{0.5}Sb_{1.5}Te_3$ films were chosen as the research target. In the previous reports, $Bi_{0.5}Sb_{1.5}Te_3$ films can only be obtained by evaporating the presynthesized $Bi_{0.5}Sb_{1.5}Te_3$ bulk materials into films by either flash evaporation[10,11] or electric current stressing.[12] The requirement for the presynthesis of bulk $Bi_{0.5}Sb_{1.5}Te_3$ and the necessitated high-vacuumed condition make above processes undesirable. All of these facts give us motivation to develop alternative synthesis process of $Bi_{0.5}Sb_{1.5}Te_3$ films. Herein, we introduced a novel process based on sequent chemical vapor transport (CVT) and the synthesized $Bi_{0.5}Sb_{1.5}Te_3$ films exhibited enhanced thermoelectric properties in comparison with previous reported $Bi_{0.5}Sb_{1.5}Te_3$ films.

In our previous work, n-type binary Bi_2Te_3 films were obtained by a simple one-stepped CVT process.[13] In this work, the synthesis of $Bi_{0.5}Sb_{1.5}Te_3$ films was accomplished by gimmicky two-stepped CVT process under the protecting carrier gas (CG). As indicated in Figure 1a, first, bismuth films were synthesized on oxidized Si substrate by a solution route, in which the precursor solution (50 mL) was composed of 0.2 mmol of $Bi(NO_3)_3$, 0.5 mmol of ethylenediaminetetraacetic acid (EDTA), and 0.5 mmol of ascorbic acid (AA) with pH about 12. Second, the Bi films were transferred into a horizontal tube furnace and placed about 20 cm downstream from the center where the Sb powder was placed, the antimony vapor was formed at ∼550 °C and transported by carrier gas to the Bi films, where the corresponding temperature was ∼320 °C to synthesize BiSb alloy films (Figure 1a, step 1). Third, the synthesized BiSb films were transferred into the horizontal tube furnace second time, placed 10 cm downstream from the center where the Te powder was placed. The tellurium vapor was formed at ∼450 °C and transported by carrier gas to the BiSb films, where the corresponding temperature was ∼410 °C to synthesize BiSbTe films (step 2). Before starting both CVT processes, the quartz tube was evacuated to $\sim 1 \times 10^{-4}$ bar and then flushed with carrier gas 3 times to prevent possible oxidation. Low-pressure ($\sim 1 \times 10^{-4}$ bar) CVT process was chosen for both steps for the reason that

Received: February 16, 2011
Accepted: April 11, 2011
Published: April 11, 2011

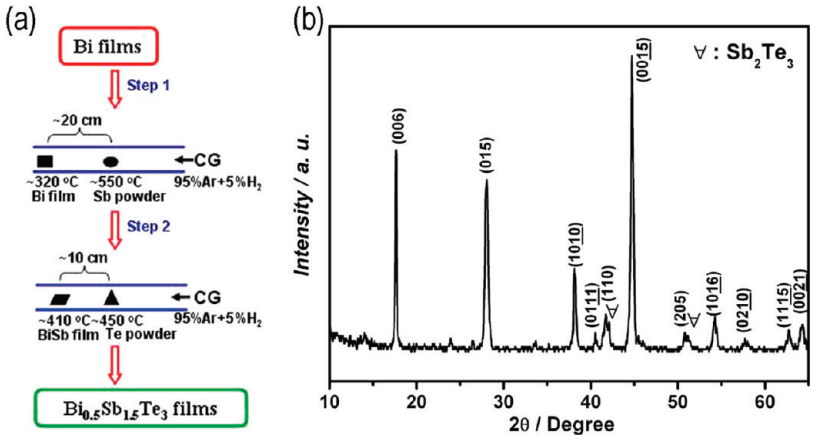

Figure 1. (a) Schematic diagram of the sequent CVT process, (b) XRD pattern of the synthesized films, indicating the main phase is $Bi_{0.5}Sb_{1.5}Te_3$ with (00L) orientation with trace amount of Sb_2Te_3.

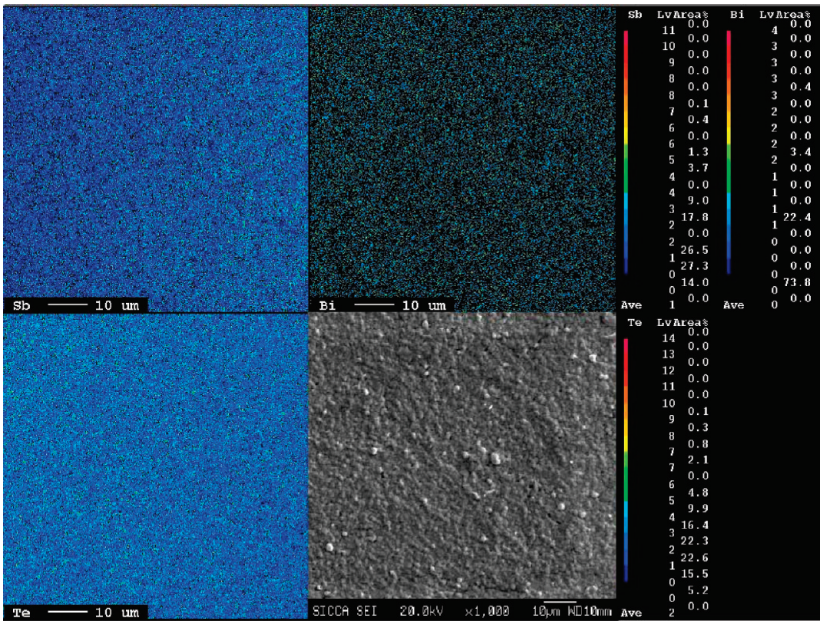

Figure 2. (a−c) Elemental distributions for $Bi_{0.5}Sb_{1.5}Te_3$ films, indicating the homogeneous distribution of the three elements (Bi, Sb, Te), (d) secondary electron image (SEI).

the chemical process at the surface of the wafers can be controlled by the reaction rate rather than the mass transfer process, and the rate-controlled CVT process will facilitate the heterogeneous nucleation and growth of the films.[14] The temperature of the substrate and vapor source played vital roles in the formation of the corresponding films. The temperature of the vapor source (including the antimony and tellurium powder) should be high enough to produce adequate vapor amount. And the temperature of the substrate should not be too high to avoid the high desorption, and then affect the nucleation and growth of the films. Besides, the temperature of Bi films in step 1 determines the synthesis of the final $Bi_{0.5}Sb_{1.5}Te_3$ products as the BiSb alloys with atomic ratio about 1:3 were only formed on the position (~320 °C) marked in step 1. If the Bi films were placed about 19 cm (~350 °C) or 21 cm (~300 °C) downstream from the center, the Bi films will overevaporate to obtain noncontinuous films with too much Sb particles (~19 cm) or be transferred into BiSb alloys with atomic ratio about 1:1 (~21 cm). The best p-type $Bi_{0.5}Sb_{1.5}Te_3$ material can not be obtained under both conditions.

As the XRD result indicated in Figure 1b (XRD measurement was taken directly from the films), the obtained films displayed rhombohedral $Bi_{0.5}Sb_{1.5}Te_3$ phase with lattice constants of $a = b = 4.295$ Å, $c = 30.26$ Å, which are consistent with the literature values ($a = b = 4.3$ Å, $c = 30.28$ Å, JCPDS 65−3674). Besides, the dominant (006) and (0015) diffraction peaks suggest that the $Bi_{0.5}Sb_{1.5}Te_3$ films have a preferred orientation along the (00*L*) planes. From the XRD result, a trace amount of Sb_2Te_3 was also detected, which might come from the Sb remains formed in Step 1. The secondary electron image (SEI) and elemental maps, including Bi, Sb, and Te, displayed in Figure 2 are uniform with no notable darker and brighter regions, which indicates that all the elements distributed homogeneously in the matrix. Quantitative analysis (see Figure S1 in the Supporting Information)

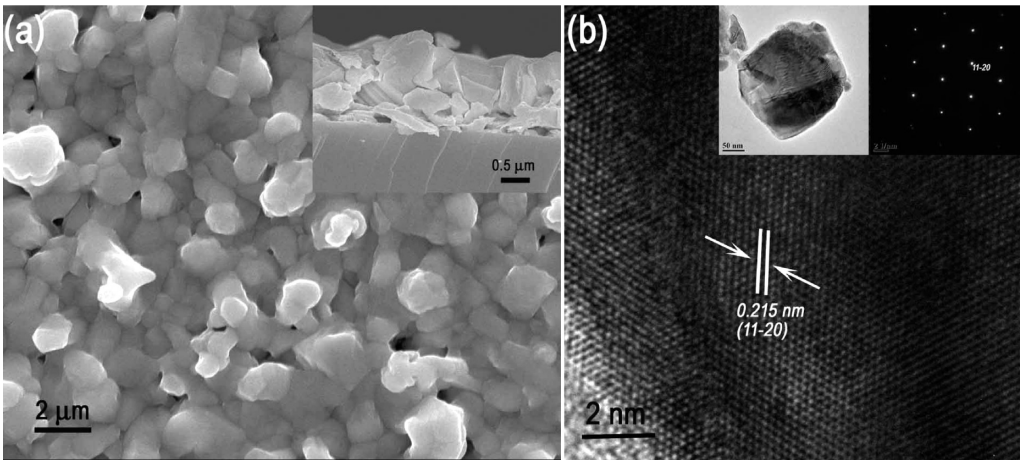

Figure 3. (a) SEM images of the $Bi_{0.5}Sb_{1.5}Te_3$ films (the inset is the corresponding cross sectional profile), (b) high-magnification TEM image of the $Bi_{0.5}Sb_{1.5}Te_3$ nanoplate (the insets are the corresponding low-magnification TEM image and the SAED pattern).

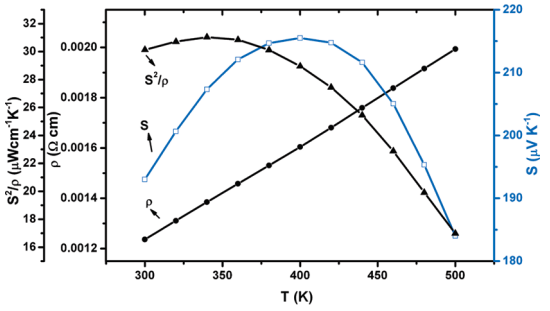

Figure 4. Temperature dependence of the electrical resistivity (●), Seebeck coefficient (□), and power factor (▲) for the $Bi_{0.5}Sb_{1.5}Te_3$ films prepared by sequent CVT process.

suggested the films are composed of bismuth, antimony and tellurium with atomic ratio of about 1:3:6, consistent with the stoichiometric proportion of bismuth antimony telluride ($Bi_{0.5}Sb_{1.5}Te_3$). From the SEM images shown in Figure 3a, the $Bi_{0.5}Sb_{1.5}Te_3$ films are constructed by platelike crystals with thickness about 1.5 μm (the inset in Figure 3a). The low magnification TEM image (the inset in Figure 3b) confirms the plate structure of the building blocks embedded in the films. The observed lattice spacing of 0.215 nm in high magnification TEM (Figure 3b) corresponds to the $(11\bar{2}0)$ plane of the rhombohedral $Bi_{0.5}Sb_{1.5}Te_3$ phase. The corresponding electron diffraction (ED) confirms the $(11\bar{2}0)$ plane of the nanoplate. Both the TEM and ED results suggest the single crystal characteristic of the nanoplate with $(00L)$ orientation, which is responsible for the $(00L)$ orientation of the films. The formation of the $(00L)$ orientations of nanoplates might be attributed to the intrinsic anisotropic structure resemblant to the hexagonal Bi_2Te_3.[15]

Figure 4 shows the temperature (T) dependence of TE transport of $Bi_{0.5}Sb_{1.5}Te_3$ films, including the electrical resistivity (ρ), Seebeck coefficient (S), and power factor (PF = S^2/ρ). Positive values of S indicate a p-type conduction, which is expected for $Bi_{0.5}Sb_{1.5}Te_3$ films. The conduction behavior (p or n character) correlates with the type of the dominant carrier. As in the A_2B_3 (A = Bi, Sb and B = Te, Se) compounds, the antisite defects dominate the carrier type and concentration.[16] In $Bi_xSb_{2-x}Te_3$, both Sb and Bi tend to form Sb_{Te} and Bi_{Te} antisites, serving as acceptors and causing p-type conduction behavior.[17] As the x value changes from 0 to 2, the carrier concentration changes from 8×10^{19} cm^{-3} to 0.5×10^{19} cm^{-3}.[18] And in the present $Bi_{0.5}Sb_{1.5}Te_3$ films, the carrier concentration, obtained from Hall effect measurement,[7] is 2.0×10^{19} cm^{-3}, which is slightly higher than the value in the $Bi_{0.5}Sb_{1.5}Te_3$ ingot[19] (1.8×10^{19} cm^{-3}) and the value in the $Bi_{0.5}Sb_{1.5}Te_3$ films[20] (1.5×10^{19} cm^{-3}) prepared by electric current stressing. This slightly higher carrier concentration might be related to the existence of the trace Sb_2Te_3 impurity. Consequently, the Seebeck coefficient for the present films at room temperature is 193 μV K^{-1}, which is lower than the value of 215 μV K^{-1} for the $Bi_{0.5}Sb_{1.5}Te_3$ ingot and 217 μV K^{-1} for $Bi_{0.5}Sb_{1.5}Te_3$ films. The maximal Seebeck coefficient reaches 216 μV K^{-1} at 400 K, and among 300−500 K, the Seebeck coefficient is above 184 μV K^{-1}, this phenomena might be related to the quantum confinement effect existed in the film that increases the difference between the Fermi level and the average mobile carrier energy.[21] From Figure 4, a linear increase in the electrical resistivity (ρ) was also indicated, suggesting the metallic conduction behavior of the present $Bi_{0.5}Sb_{1.5}Te_3$ films. The ρ at room temperature is 0.00124 Ω cm, which is lower than the value of the $Bi_{0.5}Sb_{1.5}Te_3$ films prepared by flash-evaporation (0.00164 Ω cm)[10] and electric current stressing (0.0049 Ω cm).[11] The significant enhancement of the electrical conductivity is attributed to the high carrier mobility (252 cm^2 V^{-1} s^{-1}) of the present $Bi_{0.5}Sb_{1.5}Te_3$ films, which might come from the effective interparticle contiguity with $(00L)$ oriented nanoplates embedded in the $Bi_{0.5}Sb_{1.5}Te_3$ films (Figure 1b and Figure 3). As a result, the PF researches 30 μW cm^{-1} K^{-1} at room temperature, which is much higher than the previous $Bi_{0.5}Sb_{1.5}Te_3$ films (16 μW cm^{-1} K^{-1} and 9.6 μW cm^{-1} K^{-1} for $Bi_{0.5}Sb_{1.5}Te_3$ films prepared by flash-evaporation and electric current stressing, respectively). Besides, an average PF of 27.1 μW cm^{-1} K^{-1} among the 300−500 K makes the present $Bi_{0.5}Sb_{1.5}Te_3$ films much more practical in the microheating and cooling areas, as the TE devices have a wide service temperature range.

CONCLUSIONS

In summary, sequent CVT process has been successfully applied to the synthesis of p-type $Bi_{0.5}Sb_{1.5}Te_3$ films. The films are constructed by platelike crystals with $(00L)$ orientations. As a

consequence, the PF of $Bi_{0.5}Sb_{1.5}Te_3$ films was enhanced to 30 μW cm^{-1} K^{-1} at room temperature, and the average PF of 27.1 μW cm^{-1} K^{-1} (300−500 K) makes the $Bi_{0.5}Sb_{1.5}Te_3$ films much more practical in the microheating and cooling areas, as the TE devices have a wide service temperature range.

■ ASSOCIATED CONTENT

Supporting Information. Additional figure (PDF). This material is available free of charge via the Internet at http://pubs.acs.org.

■ AUTHOR INFORMATION

Corresponding Author

*Tel.: +862152412520. Fax: +862152413122. E-mail: xhchen@mail.sic.ac.cn.

■ ACKNOWLEDGMENT

Financial support from the National Natural Science Foundation of China (50702069), Program of Shanghai Subject Chief Scientist (09XD1404400), and Shanghai Rising-Star Program (10QA1407700) are gratefully acknowledged.

■ REFERENCES

(1) Venkatasubramanian, R.; Siivola, E.; Colpitts, T.; O'Quim, B. *Nature* **2001**, *413*, 597.
(2) Harman, T. C.; Taylor, P. J.; Walsh, M. P.; LaForge, B. E. *Science* **2002**, *297*, 2229.
(3) Bottner, H.; Nurnus, J.; Gavrikov, A.; Kuhner, G.; Jagle, M.; Kunzel, C.; Eberhard, D.; Plescher, G.; Schubert, A.; Schlereth, K. H. *J. Microelectromech. Syst.* **2004**, *13*, 413.
(4) Zhao, X. B.; Ji, X. H.; Zhang, Y. H.; Zhu, T. J.; Tu, J. P.; Zhang, X. B. *Appl. Phys. Lett.* **2005**, *86*, 06211.
(5) Tang, X. F.; Xie, W. J.; Li, H.; Zhao, W. Y.; Zhang, Q. J.; Niino, M. *Appl. Phys. Lett.* **2007**, *90*, 012102.
(6) Sun, Z. L.; Liufu, S. C.; Chen, X. H.; Chen, L. D. *CrystEngComm* **2010**, *12*, 2672.
(7) Sun, Z. L.; Liufu, S. C.; Chen, L. D. *Dalton Trans.* **2010**, *39*, 10883.
(8) Jiang, J.; Chen, L. D.; Yao, Q.; Bai, S. Q.; Wang, Q. *Mater. Chem. Phys.* **2005**, *92*, 39.
(9) Poudel, B.; Hao, Q.; Ma, Y.; Lan, Y. C.; Minnich, A.; Yu, B.; Yan, X.; Wang, D. Z.; Muto, A.; Vashaee, F.; Chen, X. Y.; Liu, J. M.; Dresselhaus, M. S.; Chen, G.; Ren, Z. F. *Science* **2008**, *320*, 63.
(10) Kim, I. H. *Mater. Lett.* **2000**, *44*, 75.
(11) Takashiri, M.; Tanaka, S.; Miyazaki, K. *Thin Solid Films* **2010**, *519*, 619.
(12) Liao, C. N.; Liou, K. M.; Chen, H. S. *Appl. Phys. Lett.* **2008**, *93*, 042103.
(13) Sun, Z. L.; Liufu, S. C.; Liu, R. H.; Chen, X. H.; Chen, L. D. *J. Mater. Chem.* **2011**, *21*, 2351.
(14) Jensen, K. F.; Graves, D. B. *J. Electrochem. Soc.* **1983**, *130*, 1951.
(15) Lu, W. G.; Ding, Y.; Chen, Y. X.; Wang, Z. L.; Feng, J. Y. *J. Am. Chem. Soc.* **2005**, *127*, 10112.
(16) Cho, S.; Kim, Y.; DiVenere, A.; Wong, G. K.; Ketterson, J. B.; Meyer, J. R. *Appl. Phys. Lett.* **1999**, *75*, 1401.
(17) Miller, G. R.; Li, C. *J. Phys. Chem. Solids* **1965**, *26*, 173.
(18) Stary, Z.; Horak, J.; Stordeur, M.; Stolzer, M. *J. Phys. Chem. Solids* **1988**, *49*, 29.
(19) Lan, Y. C.; Poudel, B.; Ma, Y.; Wang, D. Z.; Dresselhaus, M. S.; Chen, G.; Ren, Z. F. *Nano Lett.* **2009**, *9*, 1419.
(20) Liao, C. N.; Chang, C. Y.; Chen, H. S. *J. Appl. Phys.* **2010**, *107*, 066103.
(21) Chen, J.; Sun, T.; Sim, D. H.; Peng, H.; Wang, H.; Fan, S.; Hoon Hng, H.; Ma, J.; Yin Chang Boey, F.; Li, S.; Kabiri Samani, M.; Chung Kit Chen, G.; Chen, X.; Wu, T.; Yan, Q. *Chem. Mater.* **2010**, *22*, 3086.